

Prognostic Value of ^{18}F -FDG PET/CT in Neoadjuvant PD-1 Inhibitor-treated NSCLC

A Five-year Follow-up Study

Xiuli Tao,* Qian Zhang,† Ning Li,‡ Shuhang Wang,‡ Wei Guo,§ Pei Yuan,|| Jianming Ying,|| Jing Li,*† Lei Guo,|| Wei Tang,† Ying Liu,* Zewei Zhang,* Shijun Zhao,† Shugeng Gao,§ and Ning Wu*†

Background: Neoadjuvant immunotherapy has shown promising short-term outcomes of perioperative treatments for resectable non-small cell lung cancer (NSCLC) and is expected to release long-term survival benefits. Here, we reported the long-term prognostic value of ^{18}F -FDG PET/CT over ~a 5-year follow-up.

Patients and Methods: A total of 35 patients with NSCLC (29 males and 6 females; median age, 62 y) received 2 doses of sintilimab, followed by complete tumor resection and PET/CT scans at baseline and post-neoadjuvant stages. We investigated the prognostic value of PET/CT for overall survival (OS) and progression-free survival (PFS), focusing on metabolic parameters of primary tumors, mediastinal lymph nodes, lymphoid organs, and immune-related adverse events on imaging.

Results: During a median follow-up of 62.6 months, patients with low primary tumor metabolism ($\text{SUL}_{\text{max}} \leq 6.6$, $\text{SUL}_{\text{peak}} \leq 4.0/3.9$, or $\text{SUL}_{\text{mean}} \leq 2.7$) at post-neoadjuvant scan were alive and disease-free, demonstrating improved OS ($P = 0.07$, 0.07 , and 0.09) and significantly enhanced PFS ($P = 0.01$, 0.02 , and 0.02); those with low metabolic tumor volume ≤ 49.3 or total lesion glycolysis ≤ 41.0 at post-neoadjuvant scan also had significantly improved OS ($P = 0.03$ and 0.05). Patients with low lymph node metabolism ($\text{SUL}_{\text{max}} \leq 4.6$) at baseline scan had significantly improved PFS ($P = 0.04$).

Conclusions: This is the first study to report the long-term prognostic value of ^{18}F -FDG PET/CT for resectable NSCLC after neoadjuvant immunotherapy. Low primary tumor metabolism at post-neoadjuvant scan and low lymph node metabolism at baseline scan are promising prognostic markers for improved clinical outcomes.

Key Words: non-small cell lung cancer, immune checkpoint inhibitors, neoadjuvant therapy, ^{18}F -FDG PET/CT, prognosis, biomarker

(*Clin Nucl Med* 2025;50:577–587)

Recent advancements in immune checkpoint inhibitors have revolutionized the treatment landscape and outcomes for metastatic non-small cell lung cancer (NSCLC) lacking oncogenic driver mutations. For patients with resectable early-stage and locally advanced NSCLC, including most stage I–II and part of stage III cases, ~30%–55% of patients develop recurrence or die of disease despite radical surgery,¹ highlighting the critical need for therapy innovation. Ongoing neoadjuvant immunotherapy trials have shown promising short-term outcomes, including safety, tolerability, and achieving major pathologic response.^{2–5} The potential benefits of neoadjuvant immunotherapy include presurgical tumor reduction, improved operability, early micrometastases elimination, prevention of distant disease, and enhanced antigen-specific T-cell response.⁶ Despite these promising short-term outcomes, long-term data and prognostic biomarkers for optimal clinical outcomes are still awaited.

To date, studies evaluating the efficacy of biomarkers for immunotherapy have focused on tumor or micro-environmental biological parameters. Despite the limitations of invasive procedures and intratumoral heterogeneity, programmed death ligand 1 expression and tumor mutational burden are important predictive and prognostic biomarkers.^{7,8} Imaging biomarkers are sometimes challenging. ^{18}F -FDG PET/CT is considered to overcome the limitations of morphologic differences and is suitable for evaluating immunotherapy efficacy.⁹ Significant associations have been observed between tumor metabolic parameters (particularly SUV_{max} or SUL_{max}) with programmed death ligand 1 expression and tumor mutational burden.^{10,11} PET/CT has also demonstrated a remarkable predictive and prognostic role for advanced NSCLC undergoing immunotherapy.^{12,13} However, the prognostic value of PET/CT in the neoadjuvant immunotherapy setting has not yet been reported.

Received for publication November 24, 2024; accepted March 20, 2025. From the *Department of Nuclear Medicine (PET-CT Center); †Department of Diagnostic Radiology; ‡Department of Clinical Trial Center; §Department of Thoracic Surgery; and ||Department of Pathology, National Cancer Center/National Clinical Research Center for Cancer/Cancer Hospital, Chinese Academy of Medical Sciences and Peking Union Medical College, Beijing, China.

Xiuli Tao and Qian Zhang contributed equally to this work and share first authorship.

Clinical Trial Registration Number: ChiCTR-OIC-17013726.

This work was supported by the National Natural Science Foundation of China (Grant number: 82001870).

Conflicts of interest and sources of funding: none declared.

Correspondence to: Ning Wu, Department of Nuclear Medicine (PET-CT Center) and Diagnostic Radiology (cjr.wuning@vip.163.com), and Shugeng Gao, Department of Thoracic Surgery (gaoshugeng@cicams.ac.cn), National Cancer Center/National Clinical Research Center for Cancer/Cancer Hospital, Chinese Academy of Medical Sciences and Peking Union Medical College, No. 17, Panjiayuan Nanli, Beijing 100021, China.

Supplemental Digital Content is available for this article. Direct URL citations are provided in the HTML and PDF versions of this article on the journal's website, www.nuclearmed.com.

Copyright © 2025 The Author(s). Published by Wolters Kluwer Health, Inc. This is an open access article distributed under the terms of the Creative Commons Attribution-Non Commercial-No Derivatives License 4.0 (<http://creativecommons.org/licenses/by-nc-nd/4.0/>), where it is permissible to download and share the work provided it is properly cited. The work cannot be changed in any way or used commercially without permission from the journal.

DOI: 10.1097/RLU.0000000000005910

The safety and short-term efficacy of neoadjuvant sintilimab for resectable NSCLC have been confirmed.³ The results particularly highlighted that metabolic parameters of PET/CT can predict the major pathologic response,¹⁴ which is considered a vital short-term endpoint with the potential to replace survival outcomes. In the current study, we investigated the prognostic value of ¹⁸F-FDG PET/CT over a 5-year period, focusing on metabolic parameters of primary tumors, mediastinal lymph nodes (LNs), lymphoid organs, and immune-related adverse events (irAEs) on imaging. To the best of our knowledge, this is the first study to report the long-term prognostic value of ¹⁸F-FDG PET/CT in patients with NSCLC undergoing neoadjuvant immunotherapy, providing a promising and imaging-derived tool for stratifying patient clinical outcomes.

PATIENTS AND METHODS

Patients

Patients in a prospective, single-center, single-arm, phase Ib trial from March 6, 2018 to March 8, 2019 were included. Among 40 patients with resectable NSCLC, 35 patients who underwent complete tumor resection and ¹⁸F-FDG PET/CT scans at baseline and post-neoadjuvant were included in the present study. Five patients were excluded; 2 of them underwent baseline PET/CT in other hospitals, and 3 did not have tumor resection after neoadjuvant therapy. The trial included treatment-naïve NSCLC at stage IA–IIIB (AJCC 8th edition) with a primary tumor diameter ≥ 2 cm. The key exclusion criteria were epidermal growth factor receptor-sensitive mutation, active autoimmune diseases, ongoing systemic immunosuppressive therapy, active and uncontrolled infection, and any other known malignant tumor. The patients received 2 doses of 200 mg intravenous sintilimab on days 1 and 22, followed by complete tumor resection and LN dissection within 29–43 days after neoadjuvant sintilimab. Consistent across all patients, PET/CT was performed at baseline scan (before neoadjuvant sintilimab administration) and post-neoadjuvant scan (following the second dose of sintilimab and within 1 week before surgery). Three adjuvant therapies were administered based on the clinical condition post-surgery and multidisciplinary committee discussions (Supplemental Table S1, Supplemental Digital Content 1, <http://links.lww.com/CNM/A554> and Supplemental Table S2, Supplemental Digital Content 1, <http://links.lww.com/CNM/A554>): (1) sintilimab monotherapy, (2) chemotherapy combined with sintilimab, or (3) conventional chemotherapy or chemoradiation therapy. The study flowchart is presented in Figure 1. This clinical trial was conducted in accordance with the Declaration of Helsinki and approved by the Ethics Committee and Institutional Review Board. All patients provided informed consent before PET/CT examinations.

¹⁸F-FDG PET/CT Acquisition and Image Analysis

Patients underwent whole-body PET/CT after intravenous administration of ¹⁸F-FDG (3.70–4.44 MBq/kg), and images were obtained ~50–70 minutes later. The difference in ¹⁸F-FDG dose between the baseline and post-neoadjuvant PET/CT scans was $<20\%$, and the uptake time was <15 minutes. PET/CT was performed using an integrated PET/CT device (Discovery 690; GE Healthcare) with spiral CT (tube voltage, 120 kV; tube current, 150 mA; slice thickness, 3.75 mm; and rotation speed, 0.8 s) in three-

dimensional mode. Images from head to thigh were obtained at 2 minutes per frame and reconstructed using the VPFX-S algorithm (2 iterations, 24 subsets, 4 mm Gaussian post-filter). A breath-hold thoracic spiral CT scan (tube voltage, 120 kV; tube current using the automatic milliamperesecond technology; slice thickness, 5 mm; and rotation speed, 0.5 s) was performed after PET/CT scan.

PET/CT images were analyzed on an Advantage Workstation (version 4.6; GE Healthcare) using PETVCAR (PET Volume Computerized Assisted Reporting), an automated segmentation software system with an iterative adaptive algorithm for detecting threshold levels. Images were retrospectively interpreted together by 2 radiologists (with 6 and 20 y of experience in thoracic tumor imaging, respectively) who were blinded to clinical data. In case of inconsistency between the 2 radiologists, a third radiologist (with more than 40 y of experience in thoracic tumor imaging) independently reviewed the images and made the final decision. Any disagreements were resolved by consensus.

Primary Tumor Metabolism and Treatment Response to Neoadjuvant Sintilimab

The volume-of-interest (VOI) of the primary tumor was auto-contoured using a three-dimensional cube that contained all FDG PET-positive areas in the axial, coronal, and sagittal planes. The following standardized uptake value lean body mass (SUL) was calculated: SUL_{max} , SUL_{mean} , SUL_{peak} , metabolic tumor volume (MTV), and total lesion glycolysis (TLG). SUL, calculated using lean body mass rather than total body weight, provides a more consistent and accurate measurement by avoiding the bias from adipose tissue, as adipose tissue metabolizes far less ¹⁸F-FDG than other tissues. It also facilitates the evaluation of treatment response according to PERCIST criteria,¹⁵ where SUL has been recommended to replace SUV. Metabolic parameters were measured by PETVCAR, which is an automated segmentation software that uses an adaptive iterative algorithm to detect the threshold level of the target volume. This adaptive iterative algorithm automatically separated the target volume from the background tissue by weighting the SUL_{max} and the SUL_{mean} with a weighting factor as a Boolean variable ($0 \leq \omega \leq 1$, where 0 = background and 1 = voxel of interest). Each voxel was assigned 0 or 1 to include or exclude it from the defined volume. The weighting factor was set at 0.5.¹⁶

The treatment response to neoadjuvant sintilimab was divided into complete metabolic response (CMR), partial metabolic response (PMR), stable metabolic disease (SMD), and progressive metabolic disease (PMD) according to the PERCIST criteria.¹⁵ Patients were classified as responders (CMR + PMR) or nonresponders (SMD + PMD).

Mediastinal Lymph Nodes Metabolism

LNs were identified in a binary manner as either positive or negative, which was clinically feasible. PET/CT-positive LNs (PET/CT-LN+) were identified as LNs with short-axis diameters ≥ 10 mm on CT component images and $SUL_{max} \geq 2.5$ on PET component images combining morphologic and functional information, which was consistent with the optimal threshold and was applied in previous studies.^{17–20} LNs with the following benign features were excluded:^{21,22} (1) lymphatic hilum, (2) benign calcification, and (3) high attenuation (nodes with higher attenuation than those of the mediastinal vascular structures

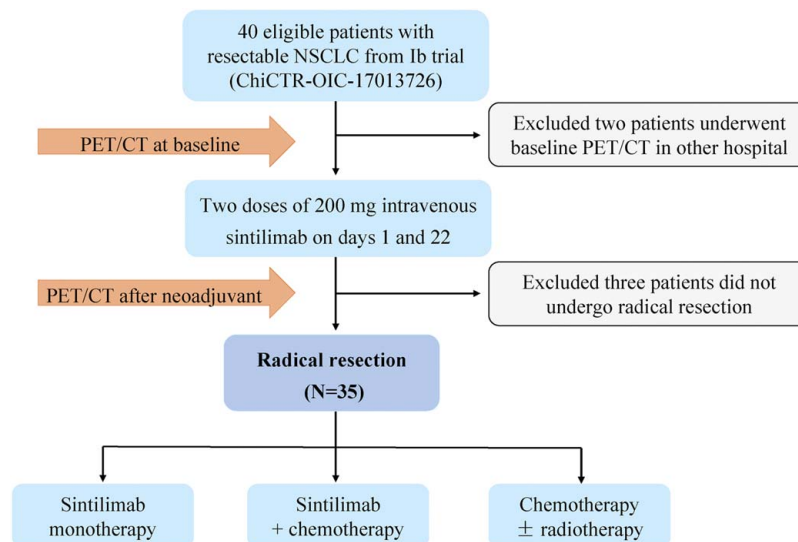


FIGURE 1. The flowchart of this study. NSCLC indicates non-small cell lung cancer.

on unenhanced CT images). Radiologists visually count the number of PET/CT-LN+ to avoid confusion caused by noise, physiological uptake, and inaccurate matching between PET and CT morphology. The number and SUL_{max} of PET/CT-LN+ for each patient were recorded. For patients who had more than one PET/CT-LN+, the highest nodal SUL_{max} was carefully measured and recorded. Unrecognizable LNs were considered as PET/CT-negative LNs (PET/CT-LN-), with the SUL values considered 0 for the analysis.

Lymphoid Organ Metabolism: Spleen and Bone Marrow Metabolism

Spleen and bone marrow metabolism were normalized using the spleen-to-liver ratio (SLR) and the bone marrow-to-liver ratio (BLR). They were calculated as the spleen SUL_{mean} divided by liver SUL_{mean} and the bone marrow SUL_{mean} divided by liver SUL_{mean} .²³ A spherical VOI of 30 mm diameter was placed on the right liver lobe, and a spherical VOI of 20 mm diameter was placed at the center of the spleen. Four spherical VOIs of 15 mm diameter were placed in the center of the L1–L4 (lumbar) vertebral bodies, whereas VOIs with vertebral fractures, metastatic lesions, hemangiomas, severe lumbar osteoarthritis, or a history of lumbar spine surgery were excluded. SUL_{mean} of the bone marrow was defined as the average SUL_{mean} of all the vertebral bodies.

Immune-related Adverse Events on PET/CT

irAEs on PET/CT refer to immunotherapy-induced organ inflammation detected on PET/CT, defined as diffuse and homogeneous organ uptake that was newly emerging or markedly increased compared with the baseline image (quantitatively, SUL_{peak} increased by >30%).²⁴ Diffuse uptake of thyroiditis, pneumonitis, mediastinal granulomatous reaction, hepatitis, pancreatitis, gastritis, colitis, cutaneous inflammation, pleuritis, osteoarticular inflammation, and other organ inflammations were collected separately. Notably, there was no correspondence between clinically reported irAEs and irAEs on PET/CT. Clinical irAEs were not the focus of the present study.

Follow-up and outcomes: Overall Survival and Progression-free Survival

Patients were followed for radiographic tumor evaluation every 3 months using contrast-enhanced CT after treatment discontinuation. Patients who did not undergo imaging at our hospital were followed up by telephone. All patients were followed up for ~5 years or until death, and the last follow-up date was December 31, 2023. In addition, MRI or contrast-enhanced CT was performed at baseline to rule out baseline brain metastases. Overall survival (OS) was defined as the time from the first sintilimab administration to the date of death from any cause. Progression-free survival (PFS) was defined as the time from the first sintilimab administration to tumor recurrence after surgery or death from any cause.

Statistical Analysis

Metabolic parameters of primary tumor, LNs, lymphoid organs, and irAEs on imaging were investigated for OS and PFS over a 5-year follow-up to determine the prognostic role of PET/CT. `Surv_cutpoint` function of the “survminer” package in R software was used to calculate the optimal cutoff value for quantitative metabolic parameters at baseline, post-neoadjuvant, and percentage variation. The metabolic parameters were dichotomized into “high” and “low” subgroups based on the optimal cutoff values. Subgroups comprising less than a quarter of patients (<8 patients) were not analyzed because unbalanced. Survival curves were generated by the Kaplan-Meier method and compared using the log-rank test. All reported P values were 2-sided, and $P \leq 0.05$ was considered statistically significant. Statistical analyses were performed using R software (version 4.0.3; packages: survival, survminer, prodlm).

RESULTS

Patient Characteristics

Among the 35 enrolled patients (29 males and 6 females; median age, 62 y), 28 (80.0%) had a history of smoking, and 29 (82.9%) were pathologically diagnosed with squamous cell carcinoma. All patients underwent surgery after neoadjuvant therapy, resulting in R0 resection

TABLE 1. Baseline Patient Characteristics (N=35)

Clinical Characteristics	Median (Range), n (%)
Age (y)	62 (48–70)
Sex	
Male	29 (82.9)
Female	6 (17.1)
Histology	
Adenocarcinoma	5 (14.3)
Squamous cell carcinoma	29 (82.9)
Mixed	1 (2.9)
Smoking history	
Never	7 (20.0)
Former or current	28 (80.0)
Pack-years	25 (0–100)
Clinical stage at baseline*	
cT (T1/2/3/4)	7 (20.0)/9 (25.7)/13 (37.1)/6 (17.1)
cN (N0/1/2)	13 (37.1)/10 (28.6)/12 (34.3)
cStage (I/II/III)	7 (20.0)/11 (31.4)/17 (48.6)
Surgical	
R0 resection	34 (97.1)
R2 resection	1 (2.9)
Surgical type	
VATS	4 (11.4)
UVATS	6 (17.1)
Open	25 (71.4)
Pathologic stage after neoadjuvant sintilimab*	
ypT (T0-1/2/3/4)	15 (42.9)/10 (28.6)/9 (25.7)/1 (2.9)
ypN (N0/1/2)	17 (48.6)/7 (20.0)/11 (31.4)
ypStage (I/II/III)	11 (31.4)/9 (25.7)/15 (42.9)
Adjuvant therapy	
Sintilimab monotherapy	15 (42.9)
Sintilimab + chemotherapy	10 (28.6)
Conventional chemotherapy ± radiotherapy	6 (17.1)
None and NA†	4 (11.4)

*Based on the criteria of the American Joint Committee on Cancer, eighth edition.

†Two patients did not receive adjuvant therapy after surgery. Two patients died a short time after the surgery because of serious adverse events.

NA indicates not available; UAVTS, uniportal video-assisted thoracoscopic surgery; VATS, video-assisted thoracoscopic surgery.

in 34 patients and R2 resection (due to mediastinal lymph node invasion) in 1 patient. Overall, 20 (57.1%) patients had pathologic stage I and II disease, 15 (42.9%) had pathologic stage III disease, 17 (48.6%) had pathologic N0, 7 (20.0%) had pathologic N1, and 11 (31.4%) had pathologic N2 after neoadjuvant therapy. In addition, 15 (42.9%) patients received sintilimab monotherapy, 10 (28.6%) received chemotherapy combined with sintilimab, and 6 (17.1%) received conventional chemotherapy or chemoradiation therapy as adjuvant treatment after surgery. Patient characteristics are summarized in Table 1.

Descriptive statistics of the quantitative parameters derived from PET/CT of the primary tumor, LNs, and lymphoid organs metabolism are summarized in Supplemental Figure S1 (Supplemental Digital Content 1, <http://links.lww.com/CNM/A554>).

At baseline scan, 14 (40.0%) patients were PET/CT-LN+ and 21 (60.0%) patients were PET/CT-LN-. There were

1, 2, and > 2 PET/CT-LN+ in 8 (22.9%), 4 (11.4%), and 2 (5.7%) patients, respectively. The median SUL_{max} of PET/CT-LN+ was 6.5 (range: 2.9–23.0). At post-neoadjuvant scan, 11 (31.4%) patients were PET/CT-LN+ and 24 (68.6%) patients were PET/CT-LN-. There were 1, 2, and > 2 PET/CT-LN+ in 6 (17.1%), 3 (8.6%), and 2 (5.7%) patients, respectively. The median SUL_{max} of PET/CT-LN+ was 5.8 (range: 2.8–8.7). Detailed information on PET/CT-LNs+ and pathologic metastatic LNs are summarized in Supplemental Table S3 (Supplemental Digital Content 1, <http://links.lww.com/CNM/A554>). At baseline scan, pathologic metastatic LNs were detected in 78.6% (11/14) of PET/CT-LN+ cases. At post-neoadjuvant scan, pathologic metastatic LNs were identified in 81.8% (9/11) of PET/CT-LN+ cases. The number of pathologic metastatic LNs after neoadjuvant immunotherapy was significantly correlated with the PET/CT-LN+ counts at baseline scan ($r = 0.525$, $P = 0.001$) and post-neoadjuvant scan ($r = 0.462$, $P = 0.005$; Supplemental Fig. S2, Supplemental Digital Content 1, <http://links.lww.com/CNM/A554>).

The metabolic responses to sintilimab according to PERCIST criteria were classified as CMR, PMR, SMD, and PMD in 0 (0%), 13 (37.1%), 21 (60.0%), and one (2.9%) of 35 patients, respectively. In addition, 37.1% (13/35) and 62.9% (22/35) patients were classified as responders and nonresponders, respectively.

Overall, 23 (65.7%) patients displayed at least one site of irAEs on PET/CT, including 9 (25.7%) with pneumonitis, 9 (25.7%) with thyroiditis, 8 (22.9%) with mediastinal granulomatous reaction, 4 (11.4%) with gastritis, 5 (14.3%) with colitis, 2 (5.7%) with cutaneous inflammation, 1 (2.9%) with osteoarticular inflammation, and 1 (2.9%) with pleuritis.

Survival Time

No patients were lost to follow-up. The median follow-up for 35 patients was 62.6 months (95% CI: 62.2–63.0), and the mean follow-up was 63.0 months (range: 1.73–70.8 mo). At the 5-year follow-up, 8 (22.9%) patients had died, with 2 deaths shortly after the surgery due to serious adverse events: disturbance of consciousness or immune-related pneumonia. Nine (25.7%) patients had tumor recurrences after surgery: 1 with local recurrence, 1 with lymph node metastasis, 1 with bone metastasis, 3 with brain metastasis, and 3 with lung metastasis. The 5-year OS rate was 76.7% (95% CI: 63.7%–92.3%), and the 5-year PFS rate was 62.3% (95% CI: 47.9%–80.9%; Fig. 2). The median OS and PFS were not reached.

PET/CT Metabolic Parameters With 5-year Overall Survival and Progression-free Survival

The prognostic value of primary tumor metabolism on PET/CT at baseline scan, post-neoadjuvant scan, and changes between the two scans were detailed based on the 5-year OS and PFS (Tables 2 and 3). The results demonstrated that only primary tumor metabolism at post-neoadjuvant scan had significant differences. All patients with low primary tumor metabolism (based on SUL_{max} ≤ 6.6, SUL_{peak} ≤ 4.0/3.9, or SUL_{mean} ≤ 2.7) at post-neoadjuvant scan survived and did not undergo tumor recurrence, showing improved OS ($P = 0.07$, 0.07, and 0.09; Figs. 3A–C) and significantly improved PFS ($P = 0.01$, 0.02, and 0.02; Figs. 3D–F). Patients with low primary tumor metabolism (based on MTV ≤ 49.3 or TLG ≤ 41.0) at post-neoadjuvant scan had significantly improved OS ($P = 0.03$ and 0.05; Figs. 4A and B).

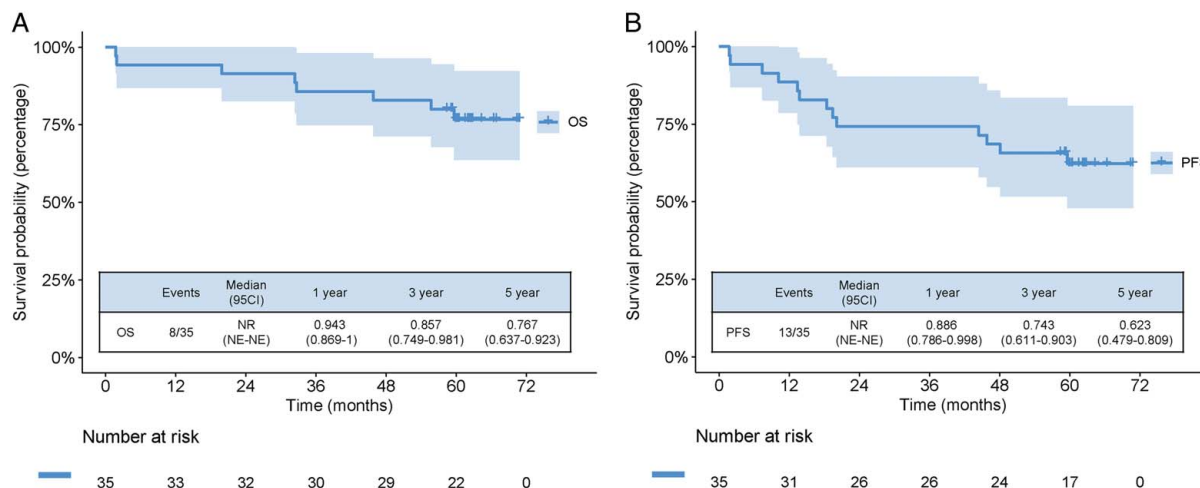


FIGURE 2. Kaplan-Meier curves of OS (A) and PFS (B) in the whole cohort for 5-year follow-up. OS indicates overall survival; PFS, progression-free survival; NE, not evaluable; NR, not reported.

Survival analyses based on the 5-year PFS indicated that the optimal cutoff of 4.6 for LN SUL_{max} at baseline scan could stratify clinical outcomes. Patients with low LN SUL_{max} (≤4.6) at baseline scan had significantly improved PFS (*P* = 0.04; Fig. 4C). The radiographic LN status revealed no significant differences between the PET/CT-LN+ and PET/CT-LN- subgroups at baseline scan (5 y OS: *P* = 0.85; 5 y PFS: *P* = 0.19; Figs. 5A and F) or post-neoadjuvant scan (5 y OS: *P* = 0.18; 5 y PFS: *P* = 0.49; Figs. 5B and G).

Survival analyses of the pathologic stage after neoadjuvant treatment revealed no significant differences between pathologic stage subgroups (5 y OS: *P* = 0.84; 5 y PFS: *P* = 0.75; Figs. 5C and H) and pathologic N stage subgroups (5 y OS: *P* = 0.98; 5 y PFS: *P* = 0.78; Figs. 5D and I).

According to the PERCIST criteria, no significant differences were observed between responders and non-responders in terms of 5-year OS and PFS (5 y OS: *P* = 0.42; 5 y PFS: *P* = 0.21; Figs. 5E and J). Nevertheless, the 5-year OS and PFS rates were higher in the responders than in the nonresponders (5 y OS rate: 83.9% vs 72.7%; 5 y PFS rate: 76.2% vs 54.5%).

No relationship was observed between lymphoid organ metabolism (SLR and BLR) and clinical outcomes (all *P* > 0.05 or not available; Tables 2 and 3).

The occurrence of irAEs on PET/CT did not significantly affect 5-year OS and PFS in overall and per-organ analyses (all *P* > 0.05; Table 4).

DISCUSSION

The safety, tolerability, and promising short-term data of neoadjuvant immunotherapy have contributed to the development of perioperative treatments for resectable NSCLC.²⁻⁵ Given the paucity of long-term data and the lack of prognostic biomarkers for optimal clinical outcomes, our study provides key insights into the prognostic value of ¹⁸F-FDG PET/CT for resectable NSCLC after neoadjuvant immunotherapy over a 5-year follow-up. The preliminary results suggest that low primary tumor metabolism at post-neoadjuvant scan and low lymph node metabolism at baseline scan are promising prognostic markers for improved clinical outcomes.

The tumor glucose uptake parameters can quantify tumor aggressiveness and disease burden by assessing the

metabolic activity (SUL values) and metabolic volume burden (MTV and TLG).^{25,26} As PET/CT at post-neoadjuvant scan served as a point of reference for residual metabolic tumor activity and burden before surgery, high tumor metabolism indicated greater residual tumor activity and burden, posing a higher risk of recurrence. Conversely, low tumor metabolism suggested reduced residual tumor activity and burden, potentially leading to durable benefits. Previous research has demonstrated the predictive value of tumor metabolism after neoadjuvant immunotherapy in relation to pathologic responses.¹⁴ Kaira et al²⁷ also demonstrated that FDG uptake after nivolumab treatment was an independent prognostic factor for predicting PFS and OS. Therefore, we revealed the clinical significance of PET/CT after neoadjuvant therapy, which seemed to be more valuable for monitoring immune response and prognosis compared with the baseline scan. Furthermore, the necessity and strategy for adjuvant therapy after surgery in the neoadjuvant immunotherapy setting remains uncertain. Patients with high tumor metabolism at post-neoadjuvant scans tend to exhibit high residual disease burden and poor prognosis. Determining whether these patients require additional adjuvant therapy after surgery is an important clinical question that requires further investigation. PET/CT merges as a promising tool for identifying candidates who may require adjuvant therapy after surgery.

As LN positivity is an important prognostic factor, we defined PET/CT-LN+ and studied the prognostic significance at baseline and post-neoadjuvant scans separately. At baseline scan, we considered that PET/CT-LN+ and FDG avidity reflected the extent of malignant LN involvement. Results indicated that the SUL_{max} of LN at baseline scan is a prognostic factor since patients with low LN SUL_{max} (≤4.6) had significantly improved PFS. Lee et al²⁸ demonstrated that a cutoff value of 4.0 provided the highest diagnostic ability for identifying malignant LNs, achieving a specificity of 94.5%. Therefore, in this study, patients with LN SUL_{max} higher than 4.6 likely indicated highly malignant LN involvement and a poor prognosis. Whether these patients require additional adjuvant therapy after surgery also warrants further investigation. Our results showed that the pathologic N stage after neoadjuvant therapy could not stratify prognosis, consistent with the finding of Endoh et al,²⁹ who

TABLE 2. Prognostic Significance of PET/CT Parameters for 5-year OS

PET/CT Parameters	Cutoff	Events for High	Events for Low	HR (95% CI)	P
Baseline scan					
Primary tumor					
SUL _{max}	16.1	1/11	7/24	0.3 (0.1–1.1)	0.18
SUL _{peak}	8.4	7/25	1/10	3.3 (0.8–14.6)	0.23
SUL _{mean}	5.5	7/23	1/12	4.3 (1.0–18.0)	0.13
MTV	57.2	4/7	4/28	—	NA*
TLG	608.6	3/4	5/31	—	NA*
LNs					
SUL _{max}	4.6	3/10	5/25	1.6 (0.3–7.3)	0.54
Lymphoid organs					
SLR	0.9	4/5	4/30	—	NA*
BLR	1.1	3/4	5/31	—	NA*
Post-neoadjuvant scan					
Primary tumor					
SUL _{max}	6.6	8/26	0/9	NA	0.07
SUL _{peak}	4.0	8/26	0/9	NA	0.07
SUL _{mean}	2.7	8/27	0/8	NA	0.09
MTV	49.3	4/8	4/27	4.1 (0.7–23.9)	0.03
TLG	41.0	8/25	0/10	NA	0.05
LNs					
SUL _{max}	0	1/11	7/24	0.3 (0.1–1.1)	0.18
Lymphoid organs					
SLR	0.8	7/24	1/11	3.8 (0.9–16.0)	0.18
BLR	0.7	7/23	1/12	4.1 (1.0–17.3)	0.15
Percentage variation ($\Delta\%$)					
Primary tumor (%)					
Δ SUL _{max} %	-18.9	6/18	2/17	3.3 (0.8–13.1)	0.12
Δ SUL _{peak} %	10.5	0/5	8/30	—	NA*
Δ SUL _{mean} %	-3.9	4/10	4/25	2.9 (0.6–14.4)	0.11
Δ MTV%	4.0	0/7	8/28	—	NA*
Δ TLG%	-23	5/14	3/21	2.9 (0.7–12.3)	0.12
LNs (%)					
Δ SUL _{max} %	-100	6/32	2/3	—	NA*
Lymphoid organs (%)					
Δ SLR%	-9.0	4/29	4/6	—	NA*
Δ BLR%	-23.1	5/31	3/4	—	NA*
Absolute metabolism change					
Primary tumor					
Δ SUL _{max}	-2.4	6/19	2/16	2.9 (0.7–11.4)	0.18
Δ SUL _{peak}	0.9	0/4	8/31	—	NA*
Δ SUL _{mean}	-0.1	4/11	4/24	2.6 (0.5–11.9)	0.17
Δ MTV	-36.0	6/32	2/3	—	NA*
Δ TLG	-694.1	6/32	2/3	—	NA*
LNs					
Δ SUL _{max}	-6.1	6/30	2/5	—	NA*
Lymphoid organs					
Δ SLR	-0.08	4/29	4/6	—	NA*
Δ BLR	-0.23	5/31	3/4	—	NA*

*Unbalanced subgroups with less than one-quarter of patients (< 8 patients) were not analyzed.

BLR indicates bone marrow-to-liver ratio; HR, hazard ratio; LNs, lymph nodes; MTV, metabolic tumor volume; NA, not available; OS, overall survival; SLR, spleen-to-liver ratio; SUL, the standardized uptake value corrected by lean body mass; TLG, total lesion glycolysis.

indicated that abnormal FDG uptake of LNs is a more efficient prognostic marker than pathologic N stage. At post-neoadjuvant scan, the radiologic evaluation of LNs is challenging owing to unique immunotherapy mechanism.³⁰ Here, radiologically abnormal uptake by LNs may not indicate a malignant involvement with pathologic responses,³¹ but rather may manifest as a phenomenon called “nodal immune flare,”³² which are deemed cancer-free and contain non-caseating granulomas. The appearance of nodal immune flares, attributed to immune activation rather than true tumor involvement, is relatively common and is not radiographically distinguishable so far. Our results indicated

that radiographic LN status and FDG avidity at post-neoadjuvant scan could not stratify patient clinical outcomes, likely attributed to the complexities in LN responses.

In our study, despite extensive collaboration with pathologists and thoracic surgeons, node-by-node matching between PET/CT-LNs and pathologic LNs proved unfeasible. This limitation stemmed from several factors: PET/CT cannot visualize all LNs, particularly smaller ones or those adjacent to tumor tissue and interlobar (eg, stations 10–14), leading to a higher number of positive LNs on pathology compared with imaging. During surgery, LNs are resected regionally by stations as a mass, rather than individually located.

TABLE 3. Prognostic Significance of PET/CT Parameters for 5-year PFS

PET/CT Parameters	Cutoff	Events for High	Events for Low	HR (95% CI)	P
Baseline scan					
Primary tumor					
SUL _{max}	11.1	11/25	2/10	2.5 (0.8–8.2)	0.21
SUL _{peak}	9.0	10/21	3/14	2.7 (0.9–8.1)	0.11
SUL _{mean}	5.5	11/23	2/12	3.6 (1.2–10.9)	0.08
MTV	21.1	10/20	3/15	3.2 (1.1–9.5)	0.06
TLG	30.1	13/31	0/4	—	NA*
LNs					
SUL _{max}	4.6	6/10	7/25	2.9 (0.8–10.8)	0.04
Lymphoid organs					
SLR	0.9	4/5	9/30	—	NA*
BLR	0.6	13/30	0/5	—	NA*
Post-neoadjuvant scan					
Primary tumor					
SUL _{max}	6.6	13/26	0/9	NA	0.01
SUL _{peak}	3.9	13/27	0/8	NA	0.02
SUL _{mean}	2.7	13/27	0/8	NA	0.02
MTV	11.0	11/23	2/12	3.3 (1.1–10.1)	0.10
TLG	26.3	13/29	0/6	—	NA*
LNs					
SUL _{max}	4.3	4/7	9/28	—	NA*
Lymphoid organs					
SLR	0.8	11/26	2/9	2.0 (0.6–6.7)	0.37
BLR	0.6	13/31	0/4	—	NA*
Percentage variation (Δ%)					
Primary tumor (%)					
ΔSUL _{max} %	-32.1	10/21	3/14	2.6 (0.9–7.7)	0.14
ΔSUL _{peak} %	10.5	13/30	0/5	—	NA*
ΔSUL _{mean} %	-57.3	11/24	2/11	3.1 (1.0–9.6)	0.12
ΔMTV%	4.0	0/7	13/28	—	NA*
ΔTLG%	-45.4	9/18	4/17	2.6 (0.9–7.7)	0.10
LNs (%)					
ΔSUL _{max} %	-77.4	10/31	3/4	—	NA*
Lymphoid organs (%)					
ΔSLR%	-9.0	9/29	4/6	—	NA*
ΔBLR%	-23.1	10/31	3/4	—	NA*
Absolute metabolism change					
Primary tumor					
ΔSUL _{max}	-5.0	10/21	3/14	2.6 (0.9–7.7)	0.14
ΔSUL _{peak}	0.9	0/4	13/31	—	NA*
ΔSUL _{mean}	-2.6	10/21	3/14	2.6 (0.9–7.7)	0.14
ΔMTV	1.7	0/5	13/30	—	NA*
ΔTLG	15.2	0/4	13/31	—	NA*
LNs					
ΔSUL _{max}	-9.5	11/32	2/3	—	NA*
Lymphoid organs					
ΔSLR	-0.08	9/29	4/6	—	NA*
ΔBLR	0.16	3/4	10/31	—	NA*

*Unbalanced subgroups with less than one-quarter of patients (< 8 patients) were not analyzed.

BLR indicates bone marrow-to-liver ratio; HR, hazard ratio; LNs, lymph nodes; MTV, metabolic tumor volume; NA, not available; PFS, progression-free survival; SLR, spleen-to-liver ratio; SUL, the standardized uptake value corrected by lean body mass; TLG, total lesion glycolysis.

Neoadjuvant therapy increases the difficulty of diagnosing LNs through both pathology and imaging. Discrepancies also arise from variations in surgical resection scope, patient positioning, and breathing motion. Consequently, we established a radiologic definition of PET/CT-LNs+ to identify target LNs for clinical focus. Our analysis revealed significant positive correlations between PET/CT-LNs+ and pathologic metastatic LNs. Though not perfect, the significant positive correlations suggest that PET/CT-LNs+ are strongly associated with pathologic metastasis, whereas PET/CT-LNs- are more likely benign. Nevertheless, efforts still need to explore objective and precise node-by-node matching between preoperative imaging and postoperative pathologic evaluation in future studies.

Kaplan-Meier analysis revealed higher 5-year OS and PFS rates in responders than those in nonresponders, however, the difference was not statistically significant. Notably, 2 responders died, neither due to tumor progression. One patient died of pneumonitis shortly after surgery, and another did not have tumor recurrence but died unexpectedly from hypoglycemia for nearly 5-year follow-up. Thus, survival benefits for responders should be considered, excluding surgical and accident-related deaths. As random events could greatly impact the results due to the limited sample size, we propose that radiologic responders may derive better survival benefits. Further investigation with a larger sample size may yield statistically significant results.

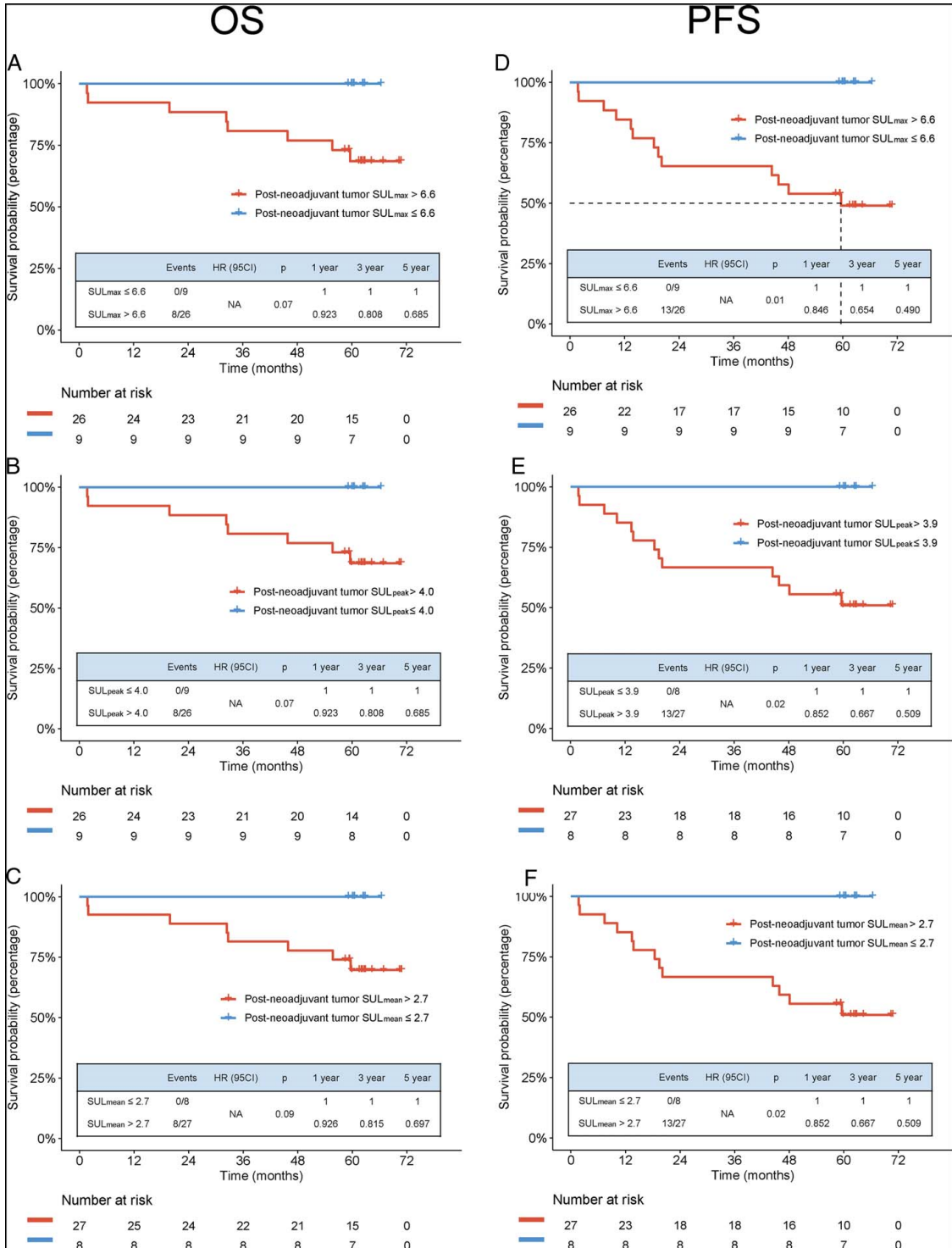


FIGURE 3. Kaplan-Meier curves of OS and PFS according to the primary tumor metabolism at post-neoadjuvant scan. **A–C,** Kaplan-Meier estimated OS according to the primary tumor SUL_{max} (**A**), SUL_{peak} (**B**), and SUL_{mean} (**C**) at post-neoadjuvant scan. **D–F,** Kaplan-Meier estimated PFS according to the primary tumor SUL_{max} (**D**), SUL_{peak} (**E**), and SUL_{mean} (**F**) at post-neoadjuvant scan. OS indicates overall survival; PFS, progression-free survival; SUL, the standardized uptake value corrected by lean body mass; NA, not available.

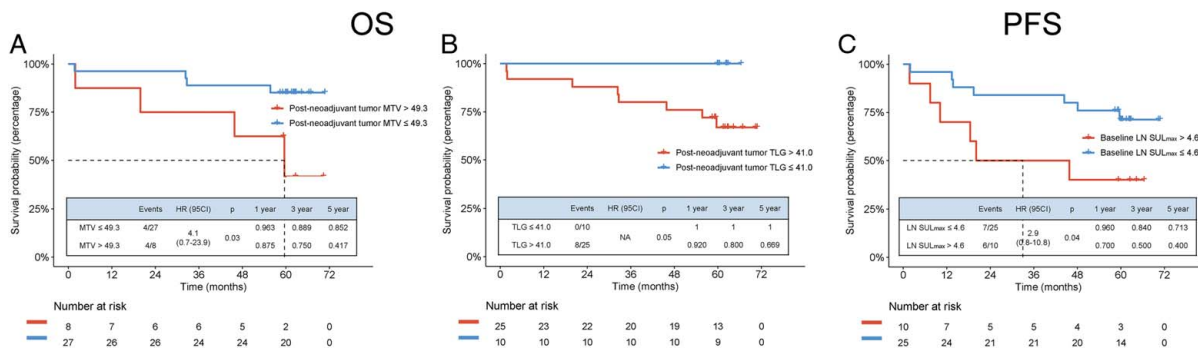


FIGURE 4. Kaplan-Meier curves of OS according to the primary tumor metabolism at post-neoadjuvant scan and PFS according to the LN metabolism at baseline scan. **A and B**, Kaplan-Meier estimated OS according to the primary tumor MTV (**A**) and TLG (**B**) at post-neoadjuvant scan. **C**, Kaplan-Meier estimated PFS according to the LN SUL_{max} at baseline scan. OS indicates overall survival; PFS, progression-free survival; MTV, metabolic tumor volume; TLG, total lesion glycolysis; LN, lymph node; SUL, the standardized uptake value corrected by lean body mass; NA, not available.

The links between cancer, inflammation, and immunosuppression are well recognized.³³ The immune response elicited in cancer-associated lymphoid tissues can be estimated on PET/CT using bone marrow and spleen FDG uptake measurements as surrogates.³⁴ Studies have confirmed that lymphoid organ metabolism, as a prognostic marker, was associated with negative clinical outcomes and systemic immunosuppression,^{34,35} as

cancer-related inflammation promotes tumor growth and malignant progression.³⁶ However, the relationship between lymphoid organ metabolism and clinical outcomes was not observed in this study, mainly because of the unbalanced subgroups with less than one-quarter of patients. Whether lymphoid organ metabolism has prognostic value in neoadjuvant immunotherapy warrants further investigation.

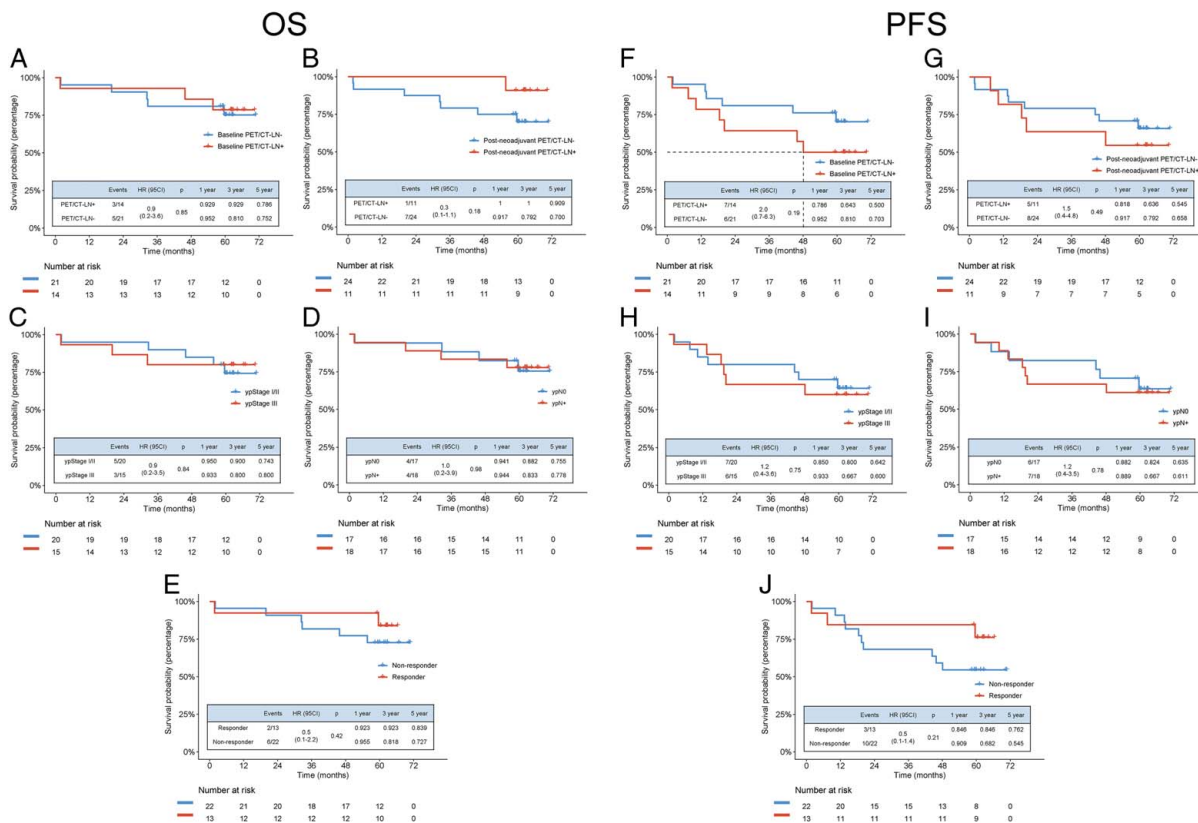


FIGURE 5. Kaplan-Meier curves of OS and PFS according to radiographic LN status, pathologic stage, and treatment response. **A–E**, Kaplan-Meier estimated OS according to radiographic LN status at baseline and post-neoadjuvant scans (**A and B**), pathologic stage after neoadjuvant sintilimab (**C and D**), and treatment response by PERCIST criteria (**E**). **F–J**, Kaplan-Meier estimated PFS according to radiographically LN status at baseline and post-neoadjuvant scans (**F and G**), pathologic stage after neoadjuvant sintilimab (**H and I**), and treatment response by PERCIST criteria (**J**). OS indicates overall survival; PFS, progression-free survival; LN, lymph node; LN+, positive lymph nodes; LN–, negative lymph nodes; NA, not available.

TABLE 4. Prognostic Significance of irAEs on PET/CT for 5-year OS and PFS

IrAEs on PET/CT	Events	5 y OS		5 y PFS	
		HR (95% CI)	P	HR (95% CI)	P
All organs*	23	0.8 (0.2–3.5)	0.73	1.0 (0.3–3.4)	0.94
Pneumonitis	9	1.8 (0.4–8.8)	0.42	2.0 (0.6–7.2)	0.21
Thyroiditis	9	0.4 (0.1–1.7)	0.33	0.9 (0.3–3.1)	0.86
Mediastinal granulomatous reaction	8	1.1 (0.2–5.4)	0.94	1.5 (0.4–5.7)	0.47
Gastritis	4	NA†	0.27	0.5 (0.1–2.5)	0.52
Colitis	5	2.0 (0.3–14.0)	0.40	1.6 (0.4–7.0)	0.48
Other organs‡	4	NA†	0.27	1.4 (0.3–7.8)	0.65

*All organs: refer to the occurrence of irAEs on PET/CT displayed at least one organ.

†Patients with gastritis and other organ inflammation were alive.

‡Other organs: 2 patients had cutaneous inflammation, 1 patient had osteoarticular inflammation, 1 patient had pleuritis.

HR indicates hazard ratio; IrAEs, immune-related adverse events; NA, not available; OS, overall survival; PFS, progression-free survival.

Immune-related organ inflammatory events are frequently detected using PET/CT in response evaluations with a relatively high detection rate,^{37,38} regardless of symptoms or not. Studies have suggested that clinical irAEs associated with more favorable efficacy and outcomes of immunotherapy, however, results remain controversial. Although inconsistency exists between clinical irAEs and those detected on PET/CT, imaging findings may precede clinical symptoms, leading to earlier therapeutic management. The prognostic value of irAEs on PET/CT has been poorly investigated. In this study, irAEs on PET/CT did not show significant prognostic value in the overall and per-organ analyses. Conversely, Humbert et al²⁴ demonstrated that immune-related gastritis on PET/CT was a novel and strong imaging biomarker for improved survival. Notably, 4 patients in the study developed gastritis on PET/CT, and none of them died. The physio-pathological explanation for the association between immune-related gastritis and improved outcomes is unclear. The role of microbiota in regulating cancer response and toxicity to immune checkpoint inhibitors could be interesting findings.³⁹

The influence of adjuvant therapy on patient prognosis remains a critical issue. In this study, 3 adjuvant therapies were administered based on multidisciplinary committee discussions with a primary focus on the postoperative pathologic staging and pathologic response (Supplemental Table S2, Supplemental Digital Content 1, <http://links.lww.com/CNM/A554>), which introduced bias in the survival evaluation. Although the preliminary results suggested no significant differences in clinical outcomes among 3 adjuvant therapies (Supplemental Fig. S3, Supplemental Digital Content 1, <http://links.lww.com/CNM/A554>), the small sample size limited the conclusion. The necessity and strategy for postoperative adjuvant therapy are currently uncertain and lack guidelines. There is a need for prospective clinical trials that formally assess the impact of various adjuvant therapies on patient outcomes. Besides, a recent study reported that adjuvant immunotherapy did not improve survival outcomes and was discouraged for unselected patients.⁴⁰ Identifying patient subgroups who are candidates for benefiting from additional adjuvant therapy is also unmet clinical need. Personalized treatment decisions require comprehensive considerations of patient condition, tumor staging, pathologic response, imaging response, surgical procedure and tumor margin, tolerability to prior therapy, and susceptibility to autoimmune toxic effects, as all these factors significantly influence the choice of adjuvant therapy strategies and clinical outcomes.

In this study with long-term survival follow-up, we first provided valuable insight into the prognostic value of ¹⁸F-FDG PET/CT in patients with NSCLC receiving neo-adjuvant immunotherapy. Nevertheless, this preliminary study has limitations. First, as our study was a phase 1b study in a single center, the sample size was relatively small with some inevitable bias. Second, based on the clinical condition and multidisciplinary committee discussion, patients have received different adjuvant therapies after surgery, which influence the survival probability. Third, a short-axis diameter ≥ 10 mm on CT images and $SUL_{max} \geq 2.5$ on PET images were artificially set as the threshold to identify PET/CT-positive LNs. However, false-positive and false-negative cases remain inevitable diagnostic challenges. The threshold requires further investigation through future large-scale studies. Finally, the optimal cutoff value for quantitative metabolic parameters was determined post hoc, and subgroup analysis of less than one-quarter of patients (<8 patients) made it difficult to compare the difference. Although this preliminary study provides valuable insights, the results should be interpreted with caution. Further studies with larger sample sizes are recommended to confirm these preliminary results, and efforts to determine the optimal cutoff values of metabolic parameters are also warranted.

CONCLUSIONS

Low primary tumor metabolism at post-neoadjuvant scan and low lymph node metabolism at baseline scan are promising prognostic markers for improved clinical outcomes. Questions remain on survival benefits and adjuvant therapy strategies to further optimize perioperative outcomes, and a recent study discouraged adjuvant immunotherapy after surgery for unselected patients.⁴⁰ Based on our findings, PET/CT is a promising tool for stratifying patient clinical outcomes and screening candidates for additional adjuvant therapy, which makes this study particularly valuable and clinical utility. These preliminary findings inform clinical decisions and provide directions for future research.

ACKNOWLEDGMENTS

The authors thank patients and their families, and the participating study teams for making this study possible.

REFERENCES

1. Uramoto H, Tanaka F. Recurrence after surgery in patients with NSCLC. *Transl Lung Cancer Res.* 2014;3:242–249.

2. Ulas EB, Dickhoff C, Schneiders FL, et al. Neoadjuvant immune checkpoint inhibitors in resectable non-small-cell lung cancer: a systematic review. *ESMO Open*. 2021;6:100244.
3. Gao S, Li N, Gao S, et al. Neoadjuvant PD-1 inhibitor (Sintilimab) in NSCLC. *J Thorac Oncol*. 2020;15:816–826.
4. Forde PM, Chaft JE, Smith KN, et al. Neoadjuvant PD-1 blockade in resectable lung cancer. *N Engl J Med*. 2018;378:1976–1986.
5. Chaft JE, Oezkan F, Kris MG, et al. Neoadjuvant atezolizumab for resectable non-small cell lung cancer: an open-label, single-arm phase II trial. *Nat Med*. 2022;28:2155–2161.
6. Burton EM, Amaria RN, Cascone T, et al. Neoadjuvant immunotherapy across cancers: meeting report from the Immunotherapy Bridge-December 1st-2nd, 2021. *J Transl Med*. 2022;20:271.
7. Rosner S, Reuss JE, Zahurak M, et al. Five-year clinical outcomes after neoadjuvant nivolumab in resectable non-small cell lung cancer. *Clin Cancer Res*. 2023;29:705–710.
8. Zhang F, Guo W, Zhou B, et al. Three-year follow-up of neoadjuvant programmed cell death protein-1 inhibitor (sintilimab) in NSCLC. *J Thorac Oncol*. 2022;17:909–920.
9. Aide N, Hicks RJ, Le Tourneau C, et al. FDG PET/CT for assessing tumour response to immunotherapy: report on the EANM symposium on immune modulation and recent review of the literature. *Eur J Nucl Med Mol Imaging*. 2019;46:238–250.
10. Seol HY, Kim YS, Kim SJ. Predictive value of ¹⁸F-fluorodeoxyglucose positron emission tomography/computed tomography for PD-L1 expression in non-small cell lung cancer: a systematic review and meta-analysis. *Thorac Cancer*. 2020;11:3260–3268.
11. Zhang Q, Tao X, Yuan P, et al. Predictive value of (18) F-FDG PET/CT and serum tumor markers for tumor mutational burden in patients with non-small cell lung cancer. *Cancer Med*. 2023;12:20864–20877.
12. Masse M, Chardin D, Tricarico P, et al. [(18)F]FDG-PET/CT atypical response patterns to immunotherapy in non-small cell lung cancer patients: long term prognosis assessment and clinical management proposal. *Eur J Nucl Med Mol Imaging*. 2024;51:3696–3708.
13. Tricarico P, Chardin D, Martin N, et al. Total metabolic tumor volume on (18)F-FDG PET/CT is a game-changer for patients with metastatic lung cancer treated with immunotherapy. *J Immunother Cancer*. 2024;12:e007628.
14. Tao X, Li N, Wu N, et al. The efficiency of (18)F-FDG PET-CT for predicting the major pathologic response to the neoadjuvant PD-1 blockade in resectable non-small cell lung cancer. *Eur J Nucl Med Mol Imaging*. 2020;47:1209–1219.
15. Wahl RL, Jacene H, Kasamon Y, et al. From RECIST to PERCIST: evolving considerations for PET response criteria in solid tumors. *J Nucl Med*. 2009;50(suppl 1):122s–150ss.
16. Moule RN, Kayani I, Prior T, et al. Adaptive 18fluoro-2-deoxyglucose positron emission tomography/computed tomography-based target volume delineation in radiotherapy planning of head and neck cancer. *Clin Oncol (R Coll Radiol)*. 2011;23:364–371.
17. Eisenhauer EA, Therasse P, Bogaerts J, et al. New response evaluation criteria in solid tumours: revised RECIST guideline (version 1.1). *Eur J Cancer*. 2009;45:228–247.
18. Hellwig D, Graeter TP, Ukena D, et al. ¹⁸F-FDG PET for mediastinal staging of lung cancer: which SUV threshold makes sense? *J Nucl Med*. 2007;48:1761–1766.
19. Wang D, Zhang X, Liu H, et al. Assessing dynamic metabolic heterogeneity in non-small cell lung cancer patients via ultra-high sensitivity total-body [(18)F]FDG PET/CT imaging: quantitative analysis of [(18)F]FDG uptake in primary tumors and metastatic lymph nodes. *Eur J Nucl Med Mol Imaging*. 2022;49:4692–4704.
20. Nagaki Y, Motoyama S, Sato Y, et al. PET-uptake reduction into lymph nodes after neoadjuvant therapy is highly predictive of prognosis for patients who have thoracic esophageal squamous cell carcinoma treated with chemoradiotherapy plus esophagectomy. *Ann Surg Oncol*. 2022;29:1336–1346.
21. Kim YK, Lee KS, Kim BT, et al. Mediastinal nodal staging of nonsmall cell lung cancer using integrated ¹⁸F-FDG PET/CT in a tuberculosis-endemic country: diagnostic efficacy in 674 patients. *Cancer*. 2007;109:1068–1077.
22. Lee JW, Kim BS, Lee DS, et al. ¹⁸F-FDG PET/CT in mediastinal lymph node staging of non-small-cell lung cancer in a tuberculosis-endemic country: consideration of lymph node calcification and distribution pattern to improve specificity. *Eur J Nucl Med Mol Imaging*. 2009;36:1794–1802.
23. Prigent K, Lasnon C, Ezine E, et al. Assessing immune organs on (18)F-FDG PET/CT imaging for therapy monitoring of immune checkpoint inhibitors: inter-observer variability, prognostic value and evolution during the treatment course of melanoma patients. *Eur J Nucl Med Mol Imaging*. 2021;48:2573–2585.
24. Humbert O, Bauckneht M, Gal J, et al. Prognostic value of immunotherapy-induced organ inflammation assessed on (18) FDG PET in patients with metastatic non-small cell lung cancer. *Eur J Nucl Med Mol Imaging*. 2022;49:3878–3891.
25. Moon SH, Hyun SH, Choi JY. Prognostic significance of volume-based PET parameters in cancer patients. *Korean J Radiol*. 2013;14:1–12.
26. Zhang ZJ, Chen JH, Meng L, et al. ¹⁸F-FDG uptake as a biologic factor predicting outcome in patients with resected non-small-cell lung cancer. *Chin Med J (Engl)*. 2007;120:125–131.
27. Kaira K, Higuchi T, Naruse I, et al. Metabolic activity by (18) F-FDG-PET/CT is predictive of early response after nivolumab in previously treated NSCLC. *Eur J Nucl Med Mol Imaging*. 2018;45:56–66.
28. Lee JW, Kim EY, Kim DJ, et al. The diagnostic ability of (18) F-FDG PET/CT for mediastinal lymph node staging using (18) F-FDG uptake and volumetric CT histogram analysis in non-small cell lung cancer. *Eur Radiol*. 2016;26:4515–4523.
29. Endoh H, Ichikawa A, Yamamoto R, et al. Prognostic impact of preoperative FDG-PET positive lymph nodes in lung cancer. *Int J Clin Oncol*. 2021;26:87–94.
30. Seymour L, Bogaerts J, Perrone A, et al. iRECIST: guidelines for response criteria for use in trials testing immunotherapeutics. *Lancet Oncol*. 2017;18:e143–e152.
31. Ling Y, Li N, Li L, et al. Different pathologic responses to neoadjuvant anti-PD-1 in primary squamous lung cancer and regional lymph nodes. *NPJ Precis Oncol*. 2020;4:32.
32. Cascone T, Weissferdt A, Godoy MCB, et al. Nodal immune flare mimics nodal disease progression following neoadjuvant immune checkpoint inhibitors in non-small cell lung cancer. *Nat Commun*. 2021;12:5045.
33. Mantovani A, Allavena P, Sica A, et al. Cancer-related inflammation. *Nature*. 2008;454:436–444.
34. Seban RD, Nemer JS, Marabelle A, et al. Prognostic and theranostic ¹⁸F-FDG PET biomarkers for anti-PD1 immunotherapy in metastatic melanoma: association with outcome and transcriptomics. *Eur J Nucl Med Mol Imaging*. 2019;46:2298–2310.
35. Lee JH, Lee HS, Kim S, et al. Prognostic significance of bone marrow and spleen (18)F-FDG uptake in patients with colorectal cancer. *Sci Rep*. 2021;11:12137.
36. Munn LL. Cancer and inflammation. *Wiley Interdiscip Rev Syst Biol Med*. 2017;9. doi: 10.1002/wsbm.1370.
37. Mekki A, Derclé L, Lichtenstein P, et al. Detection of immune-related adverse events by medical imaging in patients treated with anti-programmed cell death 1. *Eur J Cancer*. 2018;96:91–104.
38. Iravani A, Osman MM, Weppler AM, et al. FDG PET/CT for tumoral and systemic immune response monitoring of advanced melanoma during first-line combination ipilimumab and nivolumab treatment. *Eur J Nucl Med Mol Imaging*. 2020;47:2776–2786.
39. Gopalakrishnan V, Spencer CN, Nezi L, et al. Gut microbiome modulates response to anti-PD-1 immunotherapy in melanoma patients. *Science*. 2018;359:97–103.
40. Zhou Y, Li A, Yu H, et al. Neoadjuvant-adjvant vs neoadjuvant-only PD-1 and PD-L1 inhibitors for patients with resectable NSCLC: an indirect meta-analysis. *JAMA Netw Open*. 2024;7:e241285.